Turkish Journal of Electrical Engineering & Computer Sciences

http://journals.tubitak.gov.tr/elektrik/

Research Article

Turk J Elec Eng & Comp Sci
(2013) 21: 1061 – 1076

doi:10.3906/elk-1110-53

Multiobjective differential evolution-based performance optimization for switched reluctance motor drives

Hédi YAHIA,[1,*] **Noureddine LIOUANE,**[1] **Rachid DHIFAOUI,**[2]

[1]Department of Electrical Engineering, Engineering School of Monastir, Monastir, Tunisia

[2]Department of Electrical Engineering, National Institute of Applied Science and Technology, Tunis, Tunisia

Received: 25.10.2011 • **Accepted:** 05.01.2012 • **Published Online:** 03.06.2013 • **Printed:** 24.06.2013

Abstract: The simple structure, low manufacturing cost, rugged behavior, high torque per unit volume, and wide torque-speed range make a switched reluctance motor (SRM) very attractive for industrial applications. However, these advantages are overshadowed by its inherent high torque ripple, acoustic noise, and difficulty to control. The controlled parameters in SRM drives can be selected as the turn-on angle, the turn-off angle, and the current reference. This paper investigates the problem of optimal control parameters considering the maximum average torque, minimum copper losses, and minimum torque ripple as the main objectives in SRM drives. The use of evolutionary algorithms (EAs) to solve problems with multiple objectives has attracted much attention recently. Differential evolution (DE) is an EA that was developed to handle optimization problems over continuous domains. A multiobjective DE (MODE) technique is introduced here to find the optimal firing angles under multiple operating conditions. The simulation results carried out on a 4-phase 8/6 pole SRM show that the proposed MODE can be a reliable alternative for generating optimal control in the multiobjective optimization of SRM drive systems.

Key words: Optimal control parameters, differential evolution, multiobjective differential evolution, SRM drives, performance optimization

1. Introduction

In recent years, switched reluctance motor (SRM) drives have received considerable attention among researches as possible high-performance drives for many applications [1,2]. Its ability to operate in harsh environments, high torque density, and excellent torque-speed characteristics are attractive in the traction domain. However, a SRM is difficult to control. In particular, the SRM phase magnetization characteristics vary strongly as a function of the excitation current and rotor position. The magnetic circuit is saturated severely, the torque production varies nonlinearly with the rotor position, and the drive performance depends strongly on the control strategy [3–5]. Hence, there is still a need for further development in the performance optimization of SRM drives capable of operation over a large speed range [6].

High efficiency and low torque ripple are the major SRM drive characteristics designed for vehicle propulsion [7–9]. Here, we addressed these 2 performance quantities with 3 criteria for evaluating the motoring operations of SRM drives. They imply a maximum average torque, minimum copper losses, and minimum torque ripple, respectively. The effects of the turn-on and turn-off angles on these criteria are usually conflicting. Specific turn-on and turn-off angles may reduce the torque ripple, but at the cost of a lower developed torque.

*Correspondence: hedi.yahia@enim.rnu.tn

There is a need for a technique capable of finding the control parameters that achieve an optimum for the conflicting performance quantities, such as the maximum average torque, minimum copper losses, and minimum torque ripple.

In the past, many researchers have developed interesting optimization techniques for switched reluctance drives. For those techniques, control objectives were selected to maximize the average torque, to maximize the torque per root mean square (RMS) current, to maximize the efficiency, to minimize the loss, or to obtain the balance between the maximum efficiency and the minimum torque ripple [10–12]. Recently, to fulfill the best motoring operation, a multiobjective optimization function was developed by adopting a weighted sum approach [13]. This method requires multiple single-objective optimization runs with different weights for the various objectives. Usually, there can be no single optimal solution that can simultaneously satisfy all of the objectives. Pareto-based approaches, on the other hand, offer the advantage of generating multiple Pareto solutions simultaneously. In this study, the differential evolution (DE) algorithm is extended to multiobjective optimization problems using a Pareto-based approach to solve problems with multiple conflicting objectives. The approach shows promising results in SRM control. Related examples will be reported in this paper.

The remainder of this paper is organized as follows. The SRM model and motoring operation criteria are described in more detail in Sections 2.1 and 2.2. The effects of the control parameters are detailed in Section 2.3, before the previous related work in the SRM optimization techniques are presented (Section 3.1). Section 3.2 describes the proposal approach-based multiobjective DE. The simulation results are then presented in Section 4 and the conclusions drawn are given in Section 5.

2. Consideration of the SRM drive characteristics

The torque-speed characteristics of the SRM are very flexible and the adequate control-based tuning both in the turn-on and turn-off angles can effectively perform in its constant power region. Figure 1 shows the torque-speed and power-speed characteristics of the 8/6, 4 kW, 300 V SRM Oulton that has been chosen for this study. As can be seen, the highest speed of this motor in its maximum power region is more 3 times that of its base speed.

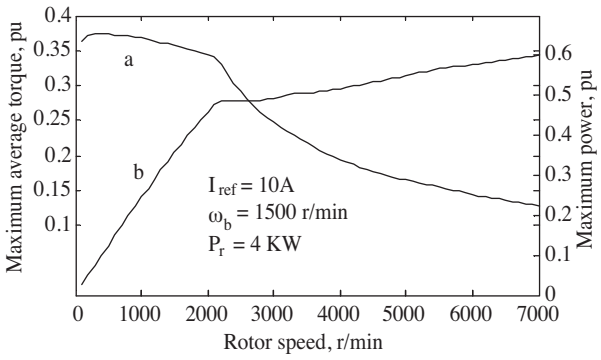

Figure 1. Simulated characteristics of the used SRM Oulton: a) torque-speed characteristics and b) power-speed characteristics.

To obtain the maximum torque, the turn-on should be set to near the minimum inductance position, as there, the current has to meet its maximum value at its maximum torque point, and the turn-off must be at about the maximum inductance position [14]. To prevent negative torque production and any loss of positive torque production, the turn-off should be carefully chosen. Thus, an optimization problem arises concerning the

both turn-on and turn-off for a higher speed range in the constant power region for SRM drives. This region is very important for industrial applications like electric vehicles [4].

2.1. SRM model

As previously indicated, the SRM used in this paper has 8 stator teeth, 6 rotor teeth, and 4 phases. It is assumed that the machine is balanced and symmetrical, the mutual phase coupling is negligible, and that the hysteresis and eddy currents are absent. Some approaches taking these factors into account were reported in [15–17]. The voltage across each phase winding j is equal to the sum of the resistive voltage drop and the rate of the flux linkages, and is given by:

$$V_j(t) = Ri_j(t) + \frac{d\varphi_j(\theta, i)}{dt}. \tag{1}$$

In SRM, the coenergy $W'$is equal to the area enclosed by the curve of the flux linkage versus the current over an exercitation cycle, and can be expressed for the jth phase by:

$$W'_j(\theta, i) = \int_0^i \varphi_j(\theta, i) d\ i_j|_{\ \theta = cons\tan t}. \tag{2}$$

For the case of constant excitation, the electromagnetic torque produced by each phase can be obtained from the derivative of the coenergy versus the rotor displacement as:

$$T_{ej}(\theta, i) = \frac{\partial W'_j(\theta, i)}{\partial \theta}\ |_{i = cons\tan t}. \tag{3}$$

The total instantaneous torque is given by the sum of the individual phase torques as follows for the considered SRM:

$$T_e = \sum_{j=1}^{4} T_{ej}(\theta, i), \tag{4}$$

and the average torque can be derived mathematically by integrating Eq. (4) over an electrical cycle as follows:

$$T_{avg} = \frac{1}{2\pi} \int_0^{2\pi} T_e d\theta. \tag{5}$$

Integrating Eq. (1) over a time period τ, the flux linkage is given by:

$$\varphi(t) = \varphi(0) + \int_0^{\tau} [V(t) - Ri(t)]\, dt. \tag{6}$$

An improved indirect measurement method, based on the data acquisition system developed for the digitized characterization of the flux linkage, was used to determine the flux linkage versus the current data. It consists of winding a sense coil around the stator teeth of the fed phase and then measuring the induced voltage. The flux is deduced from the measured induced voltages off-line. Furthermore, a numerical method is presented that permits the compensation of the effects of the current ripple. The measured static data perfectly characterize

the motor and are used in the performance optimization for the machine drives. The measured flux linkage and static electromagnetic torque versus the current under the rotor angles for the studied SRM are shown in Figures 2a and 2b, respectively. The instantaneous current of the winding is deduced by the inversion of the measured static data. The flux linkage at any instant can be obtained by calculating Eq. (6), using an adequate digital integration technique and voltage sensor. Next, the instantaneous induced electromagnetic torque is determined from the static torque table for the current corresponding to the obtained curve of the flux linkage under the rotor positions.

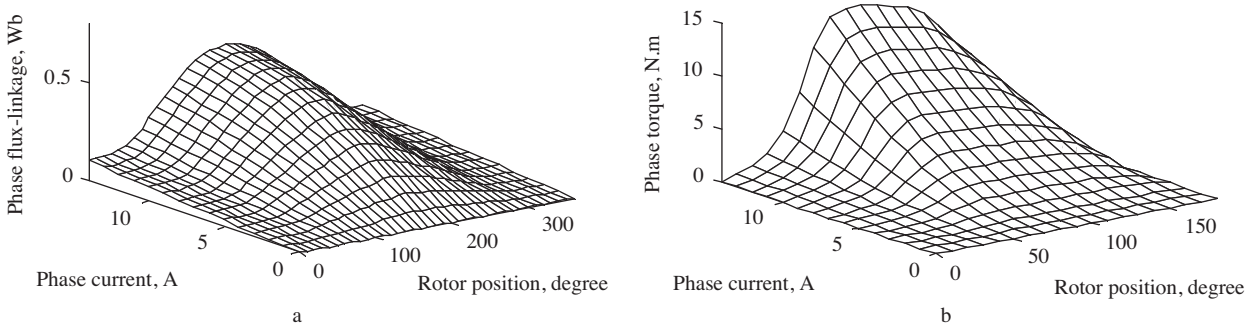

Figure 2. SRM magnetization characteristics of: a) measured phase flux linkage and b) phase static electromagnetic torque.

2.2. Criteria

The multiobjective optimization technique introduced in this paper is based on 3 criteria to evaluate the motoring operations. They are the maximum average torque, the minimum copper losses, and the minimum torque ripple.

The SRM average-torque maximization returns to maximize the average torque developed by each phase during one electrical cycle at a fixed speed and current limit condition. Hence, by adjusting the turn-on and turn-off at a given speed and under a current reference, the instantaneous torque area changes, as shown in Figure 3. We notice that the average torque increases with an increase in the area under its instantaneous torque curve. Thus, more average torque can be achieved by allowing a negative phase torque, and, consequently, a higher phase current, which leads to the generation of more copper losses and a high-torque ripple factor [1].

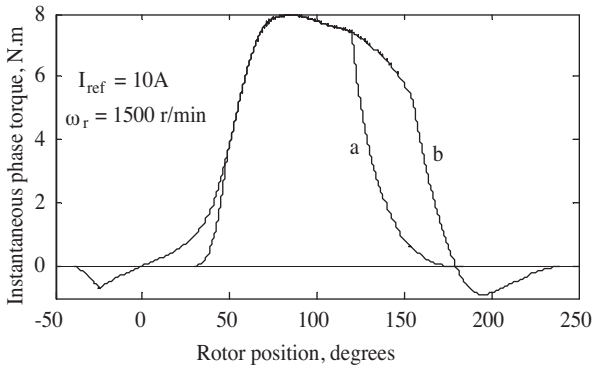

Figure 3. Comparison of instantaneous torque areas: a) curve obtained with $\theta_{on} = 30^\circ$ and $\theta_{off=120^\circ}$ and b) curve obtained with $\theta_{on} = -35^\circ$ and $\theta_{off=150^\circ}$.

Based on the multiobjective optimization, we consider the copper losses and torque ripple as the main criteria, as well as maximum average torque.

The copper loss depends on the RMS stator current and is given by:

$$P_{cu} = 4I_{rms}^2 R. \tag{7}$$

The torque ripple is defined by the normalized torque deviation with respect to the average torque. This corresponds to the following coefficient, K_T, calculated over a cycle:

$$K_T = \frac{T_{e\max} - T_{e\min}}{T_{avg}}. \tag{8}$$

2.3. Effects of the control parameters

Investigating the effects of the controlled parameters on the criteria is conducted for several combinations of turn-on and turn-off when the SRM is operating at a fixed speed and a given current reference. Figure 4a illustrates the effect of the control angles on the torque criterion for a rotor speed of 1500 r/min and a current reference of 10 A. There are optimal turn-on and turn-off angles maximizing the developed torque. The effect of the control angles on the torque ripple factor criterion is depicted in Figure 4b for the same rotor speed and current reference. The minimum torque ripple factor can be reached according to the optimal turn-on and turn-off angle combination. Figure 4c shows the effect of the turn-on and turn-off angles on the copper losses criterion at 1500 r/min and 10 A for the motor speed and current reference, respectively. This characteristic is monotone and the global minimum cannot be clearly observed. Minimizing the copper loss can be regarded as maximizing the average torque per RMS current.

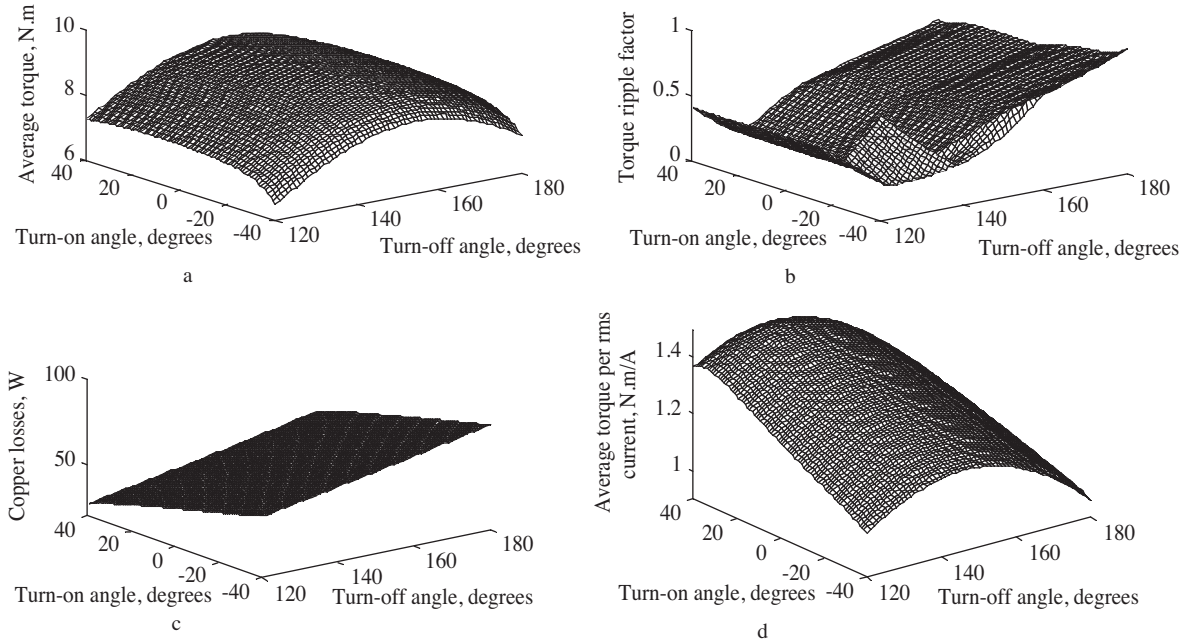

Figure 4. Effects of the control angles at 1500 r/min and I_{ref} = 10A of: a) average torque, b) torque ripple factor, c) copper loss, and d) average torque per RMS current.

Consequently, the average torque per RMS current can be expressed by Eq. (9) and the effect of the turn-on and turn-off angles is illustrated in Figure 4d at 1500 r/min and 10 A for the motor speed and current

reference, respectively. The maximum average torque per RMS current is clearly detected and the optimal control angles are found.

$$TP = \frac{T_{avg}}{I_{rms}} \tag{9}$$

Various simulations are conducted in the entire speed range for the maximization of the average torque, minimization of the torque ripple, and maximization of the average torque per RMS current and the optimization results are compared in Figures 5, 6, and 7, respectively. The optimal control parameters, θ_{on}^{opt} and θ_{off}^{opt}, according to the drive criteria at a selected speed are recapitulated in Table generated for a current reference of 10 A.

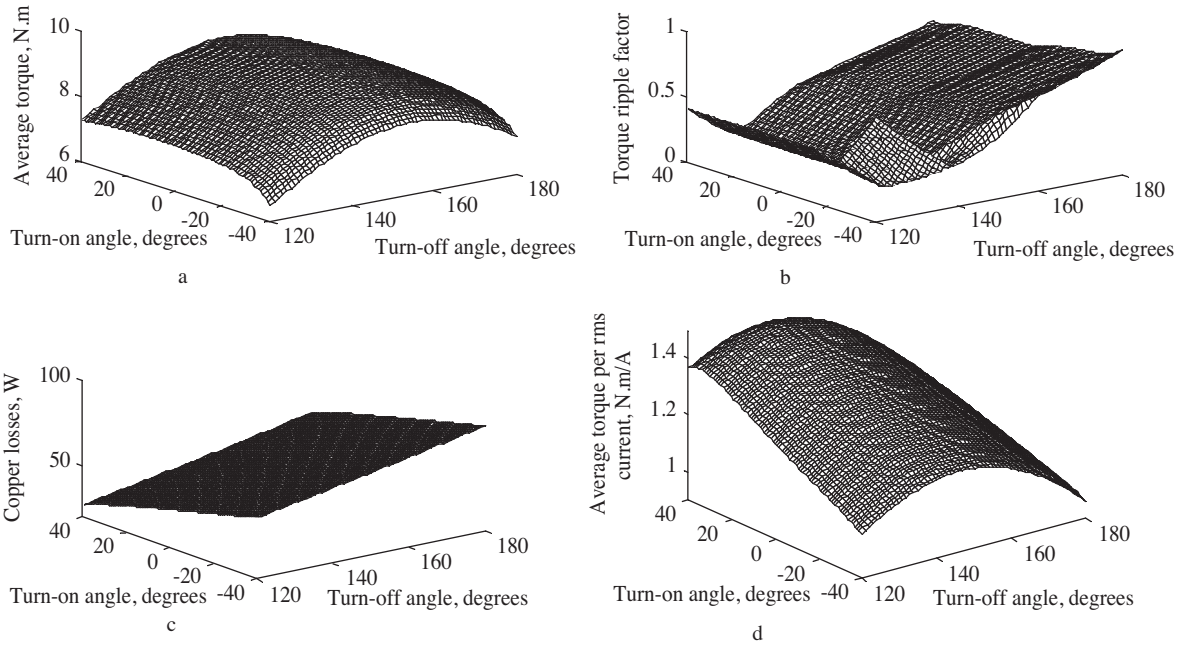

Figure 5. Comparison of torque-speed curves.

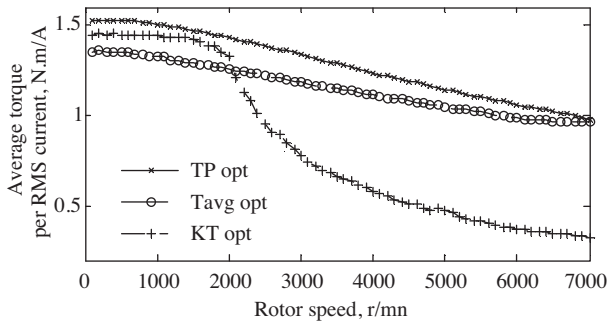

Figure 6. Comparison of the average torque per RMS current-speed curves.

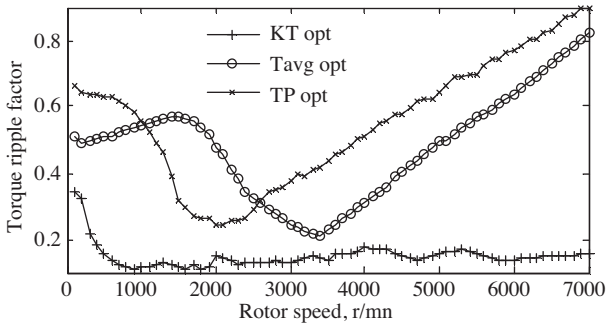

Figure 7. Comparison of torque ripple factor-speed curves.

The performance optimization leads to high calculation times (the processing time required to generate the solution was more than 2 h on a Pentium Core 2 Duo) and there is not a single solution that optimizes

all of the criteria. The problem drive can be formulated in multiobjective optimization. Hence, the field of multiobjective optimization deals with the simultaneous optimization of multiple conflicting objective functions.

Table. Optimal control angles at the corresponding criteria.

Criteria ω, r/min	T_{avg}, N.m		TP, N.m/A		K_T	
	θ_{on}^{opt}, degree	θ_{off}^{opt}, degree	θ_{on}^{opt}, degree	θ_{off}^{opt}, degree	θ_{on}^{opt}, degree	θ_{off}^{opt}, degree
500	–3	171	44	158	43	136
1000	–6	163	39	149	34	132
1500	–9	155	34	140	34	132
2000	–13	147	28	133	37	135
2500	–15	140	21	128	40	136
3000	–19	133	13	122	41	136
5000	–32	111	–13	105	39	135
7000	–39	96	–36	93	41	136

2.4. Control strategies

To avoid difficulties in obtaining the analytical derivatives for the severely nonlinear SRM, numerical optimization techniques may be favored [18]. Based on these equations and the measured characteristics of the flux linkage and static torque, we have developed a simulation function in a MATLAB environment with M-file scripts. This function delivers the average torque, average torque per RMS current, and torque ripple as a function of the turn-on angle, turn-off angle, reference current, phase voltage, winding resistance, angular velocity, and SRM measured characteristics in the form of:

$$[T_{avg}, TP, K_T] = Function\_Optimisation\ (\theta_{on}, \theta_{off}, I_{ref}, V, R, \omega, SRM\_mc)\,.$$

In order to achieve a high performance, the SR motor should be operated with variable commutation angles. Various researchers have elaborated on the performance of SRMs with angle control, but there is little guidance for choosing these angles that does not involve direct experimental search or computationally intensive numerical optimization.

2.5. Existing techniques

From the available literature, it is observed that conventional a priori guidance-based numerical optimization techniques, as alternatives to circumvent the difficulties in obtaining the analytical derivatives of the objective functions, may only offer a local optimum and are usually appropriate for single-objective optimization [19]. The computationally intensive numerical optimization belongs to an a posteriori guidance search method that can find the best solution after all of possible trials have been conducted [20]. An example of applying such a technique for finding the optimal control angles for the maximum average torque, maximum torque per copper loss, and minimum torque ripple under a predetermined operating condition is presented in Section 2.3. Here, we note that this technique is only applied to single-parameter optimization. The maximum average torque and minimum loss criteria are performed by a response surface methodology [20]. The optimization algorithm acts on 2 steps. The maximum average torque angles are determined in the 1st step and these results are used as starting points in the 2nd step, which optimizes the switching angles on the minimal losses in the windings. However, these performance quantities are sequentially optimized, one at a time. Mainly due to the inability of these methods in multidimensional performance optimization, a practical search method, by mapping the

performance quantities in the final map, is used to determine the optimum firing angles for achieving the highest drive efficiency with a lower torque ripple in a 102-kW SRM drive [21]. The manual search, by trial and error, is implemented in a genetic algorithm (GA) and is also applied to Pareto multiobjective optimization [22]. Pareto-optimal firing angles are developed for efficiency and torque maximization [18].

Recently, control angles have been optimized to maximize the multiobjective function developed for motoring the torque, copper loss, and torque ripple criteria using 3 weight factors [23]. This method follows a preference-based approach, where a relative preference vector is used to scalarize the multiple objectives. The outcome of using classical searches and optimization methods uses a point-by-point approach, where one solution in each of the iterations is modified to a different solution as a single optimized solution [24]. Achieving a set of Pareto-optimal control angles for a high motoring torque, high torque per RMS current, and low torque ripple avoids a precommitment on weighting the performance objectives. However, evolutionary algorithms (EAs) can find multiple optimal solutions in a single simulation run due to their population-based search approach [25]. In this paper, a multiobjective DE (MODE) is applied to SRM performance optimization problems.

2.6. Multiobjective differential evolution-based method

Mathematical programming techniques have certain limitations when tackling multiobjective optimizations (MOPs), such as most of them cannot find multiple solutions in a single run, and the multiple application of these methods does not guarantee finding widely different Pareto-optimal solutions [26–28]. However, EAs deal simultaneously with a set of possible solutions that allows for the finding of several members of the Pareto-optimal set in a single run of the algorithm [29]. Additionally, EAs are less susceptible to the shape or continuity of the Pareto front [30].

The DE algorithm is a novel EA for faster optimization, of which the mutation operator is based on the distribution of the solutions in the population [31]. DE is a simple yet powerful population-based direct search algorithm with a generation-and-test feature for globally optimizing functions using real valued parameters. While a conventional GA uses binary coding to represent problem parameters, it sometimes uses integer or real number representation as well [32]. The DE algorithm utilizes NP (population size) and D-dimensional vectors as a population for each iteration (called a generation of this algorithm).

$$X_i = (x_{i1}, ..., x_{in})^T \;\; i = 1, ..., NP$$

The initial NP D-dimensional vector is chosen randomly and should cover the entire parameter space X_i^0

$$X_i^0 = lower(x_i) + rand_i[0,1] \times (upper(x_i) - lower(x_i))$$

At each generation, 2 operators, namely the mutation and crossover, are applied to each individual, thus producing the new population. Next, a selection phase takes place, where each individual of the new population is compared to the corresponding individual of the old population, and the best between them is selected as a member of the population in the next generation [31]. According to the mutation operator, for each individual X_i^G, $i = 1, ..., NP X_i^G$, $i = 1, ..., NP$ at generation G, a mutation vector,

$$V_i^{(G+1)} = \left[v_{i1}^{(G+1)}, v_{i2}^{(G+1)}, ..., v_{in}^{(G+1)} \right]^T,$$

is determined using Eq. (10). The choice of Eq. (10) dictates the variant of DE to be used in the application:

$$V_i^{(G+1)} = X_{best}^{(G)} + F\left(X_{r1}^{(G)} - X_{r2}^{(G)}\right), \tag{10}$$

where $X_{best}^{(G)}$ is the best individual of the population at generation G, $F \geq 0$ is a real parameter, called the mutation constant that controls the amplification of the difference between 2 individuals so as to avoid search stagnation, and $r1$ and $r2$ are mutually different integers, randomly selected from the set $\{1, 2, ..., i-1, i+1, ..., NP\}$.

Following the mutation phase, the crossover operator is applied to the population. For each mutant vector, $V_i^{(G+1)}$, an index $rnbr(i) \in \{1, 2, ..., n\}$ is randomly chosen, and a trial vector

$$U_i^{(G+1)} = \left[u_{i1}^{(G+1)}, u_{i2}^{(G+1)}, ..., u_{in}^{(G+1)}\right]^T$$

is generated with:

$$u_{ij}^{(G+1)} = \begin{cases} v_{ij}^{G+1} if\,[randb(j) \leq CR]\, or\, [j = rnbr(i)] \\ x_{ij}^{G} if\,[randb(j) > CR]\, and\, [j \neq rnbr(i)] \end{cases}, \tag{11}$$

where $j = 1, 2, \ldots, n$; rand b(j) is the jth evaluation of a uniform random number generator within [0,1]; and CR is the user defined crossover constant in the range of [0,1] [31].

To decide whether the vector $U_i^{(G+1)}$ should be a member of the population of the next generation, it is compared to the corresponding vector X_i^G. Thus, if f denotes the objective function to minimize, then:

$$X_i^{(G+1)} = \begin{cases} U_i^{G+1} iff(U_i^{G+1}) < f(X_i^G \\ X_i^G otherwise \end{cases}. \tag{12}$$

Therefore, each individual of the trial vector is compared with its parent vector and the better one is passed to the next generation.

DE has been applied successfully to a wide range of single optimization problems [33]. Hence, several researchers have tried to extend it to handle MOPs. In single-objective optimization, the decision is easy: the candidate replaces the parent only when the candidate is better than the parent. In MOPs, on the other hand, the decision is not so straightforward due to the set of optimal solutions, and the selection procedure has to be modified.

In the literature, many algorithms are used to find multiple nondominated fronts like the naïve and slow method [34], fast and efficient method [35], and Kung et al.'s method [36]. Recently, 2 new algorithms were proposed by Mishra [37] and Jun Du [38]. In this study, we use the sorting-based algorithm proposed by Jun Du for finding the undominated set in the multiobjective optimization selection scheme extended to the traditional DE. According to Jun Du, his algorithm is better than Kung's algorithm. Through the selection scheme, the strategy used to solve the multiobjective performance optimization for SRM drives is *DE/best/1/bin*. It operates like the classical DE, except that the base vector is selected from the best vector among the population and the other 2 individuals are selected randomly. *DE/best/1/bin* starts by defining and evaluating the initial population through calculating the fitness value for each individual. After that, until the termination condition is not reached, the necessary individuals are picked, and a new one is produced according to the selected DE

scheme [39]. This new individual is evaluated and compared with the old one. Only the one with the best fitness value will be chosen and pass for population of the next generation. The pseudo-code of the selected DE scheme is presented in Figure 8 and the working principle of the proposed MODE algorithm is given in Figure 9.

Begin

(1) Initialize the population

(2) Evaluate the initial population

(3) Wile termination condition is not satisfied

Do

. Randomly select individual $X_{r1} \neq X_{best}$
. Randomly select individual $X_{r2} \neq X_{r1}$ and $\neq X_{best}$
. Generate trial individual: $X_{trial} = X_{best} + F(X_{r1} - X_{r2})$
. Use C_r to define the amount of genes changed in trial individual
. Evaluate the trial individual
. Deterministic selection

End While
End

Figure 8. Pseudo-code for *DE/best/1/bin* scheme.

3. Simulation results

The turn-on and the turn-off angles can be used to control the average torque, average torque per copper loss, and torque ripple when the SRM is operating at a fixed speed and for a given current reference. However, it can be observed from Section 2.3 that the turn-on and turn-off angles have different optimal values, respectively, to optimize the average torque, the average torque per copper loss, or the torque ripple factor. It is impossible to simultaneously optimize those 3 objectives. There are 3 conflicting objectives that need to be optimized simultaneously. The field of multiobjective optimization deals with the simultaneous optimization of multiple competing objective functions. Hence, we consider a multiobjective problem of the form:

Maximize

$$f_1 = T_{avg}(\theta_{on}, \theta_{off})$$

Minimize

$$f_2 = K_T(\theta_{on}, \theta_{off})$$

Maximize

$$f_3 = TP(\theta_{on}, \theta_{off})$$

Two decision variables, namely the turn-on angle and turn-off angle, are considered for optimization. Their bounds are:

$$-45^\circ \leq \theta_{on} \leq 45^\circ$$
$$100^\circ \leq \theta_{off} \leq 190^\circ$$

Begin

1. Initialize the set of MODE parameters (D, NP, CR, F, and NG).
2. Specify SRM criteria.
3. Specify the SRM measured characteristics.
4. Generate randomly control angles (θ_{on} and θ_{off}) with uniform distribution and respecting the constraint $\theta_{on} \langle \theta_{off}$

   $X_i^G = \begin{bmatrix} \theta_{on-i} \\ \theta_{off-i} \end{bmatrix}$, where i =1, 2, ... NP.
5. Generate random vector $X_{best}^G = \begin{bmatrix} \theta_{on-best} \\ \theta_{off-best} \end{bmatrix}$ and compute its performance by MATLAB function.
6. While stopping criterion is not satisfied
   DO

   . Select randomly 2 integer $r_1 \neq r_2 \in (1, NP)$ and $X_{r1}^G = \begin{bmatrix} \theta_{on-r1} \\ \theta_{off-r1} \end{bmatrix}$, $X_{r2}^G = \begin{bmatrix} \theta_{on-r2} \\ \theta_{off-r2} \end{bmatrix}$.

   . Compute the mutant vector $V_i^G = X_{best}^G + F\left(X_{r1}^G - X_{r2}^G\right)$.

   . Apply the crossover operator and compute the trial vector:

   $U_i^G = \begin{cases} V_i^G \; if(jrand(j) \leq CR) or j = Rnbr(i) \\ X_{best}^G otherwise \end{cases}$

   . Apply the selection mechanism by evaluating the objective functions $f(U_i^G)$:

   if $f(U_i^G) \leq f(X_{best}^G)$

   $select U_i^G, the trial vector$

   $X_i^{G+1} = U_i^G$

   $else$

   $X_i^{G+1} = X_{best}^G$

   End While.
7. Remove the dominated solutions from the last generation using the Jun Du algorithm [36].
8. Output the set of nondominated solutions.

End

Figure 9. Pseudo-code for MODE algorithm.

One constraint is also considered for optimization:

$$\theta_{on} \langle \theta_{off},$$

at a fixed speed and for a given current reference.

The proposed MODE algorithm is coded in MATLAB 7.6 and the results obtained through the simulation are discussed below. The following parameters are used while applying the MODE algorithm. The initial population was set to 90, CR = 0.3, mutation constant $F = 0.5$, and the maximum number of generations = 600.

Figure 10 shows the undominated solutions for the SRM drive when maximizing the average torque and average torque per RMS current and minimizing the torque ripple. The algorithm gives a good spread of the solution, maintaining the diversity and convergence, and offering more potential solutions to choose from.

The easiest way to approve the computed results with the real Pareto solution is to plot the Pareto solutions obtained in the 2-dimensional objective plane. The maximizing average torque is plotted against the minimizing torque in Figure 11, whereas the maximizing torque per RMS current versus the minimizing torque ripple is shown in Figure 12. The MODE method produces quality undominated solutions along the Pareto front. This proves that the MODE performs well on real-world engineering systems.

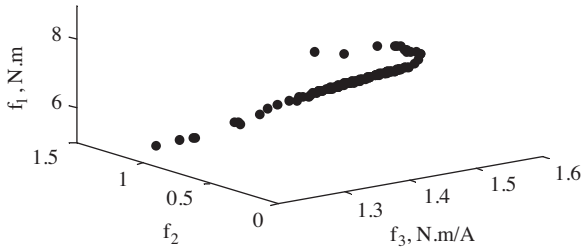

Figure 10. Pareto-optimal solutions using the MODE algorithm involved in the 3-dimensional objective space.

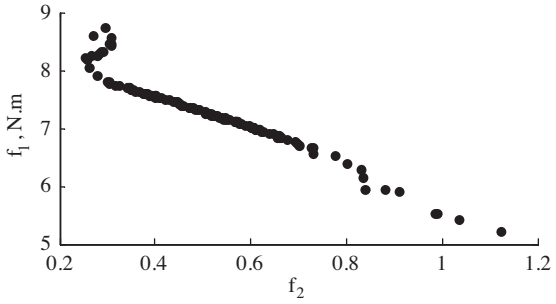

Figure 11. Pareto front in the 2-dimensional objective plane of maximizing torque versus minimizing torque ripple.

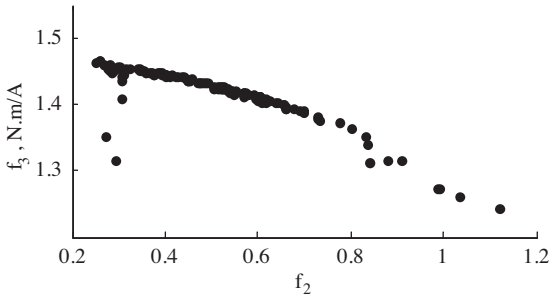

Figure 12. Pareto front in the 2-dimensional objective plane of maximizing torque per RMS current versus minimizing torque ripple.

Figure 13 shows the decision variables θ_{on} and θ_{off} plotted against the objective functions. The decision maker can choose any desired solution of his/her interest from the broad range of solutions available.

In order to demonstrate the effectiveness of the proposed algorithm for SRM drives, the results of a typical simulation run with the MODE*/best/1/bin* algorithm and multiobjective GA (MOGA) are shown in Figure 14. To apply the MODE algorithm, the following parameters are used. The initial population is set to 90, CR = 0.3, mutation constant $F = 0.5$, and the maximum number of generations = 600. For the MOGA, the initial population is set to 90, the crossover probability = 0.85, and the mutation probability = 0.02. This algorithm is also run for 600 generations. It can be clearly seen that the MODE achieves better Pareto-optimal solutions compared to the MOGA. Another comparison was made with respect to the actual processing time and function calls for a given population size. As shown in Figure 15, the 2 methods were compared at population sizes of 150, 300, 500, 700, and 1000. For all of the population sizes, it can be clearly seen that the MOGA eventually required more processing time than the MODE algorithm.

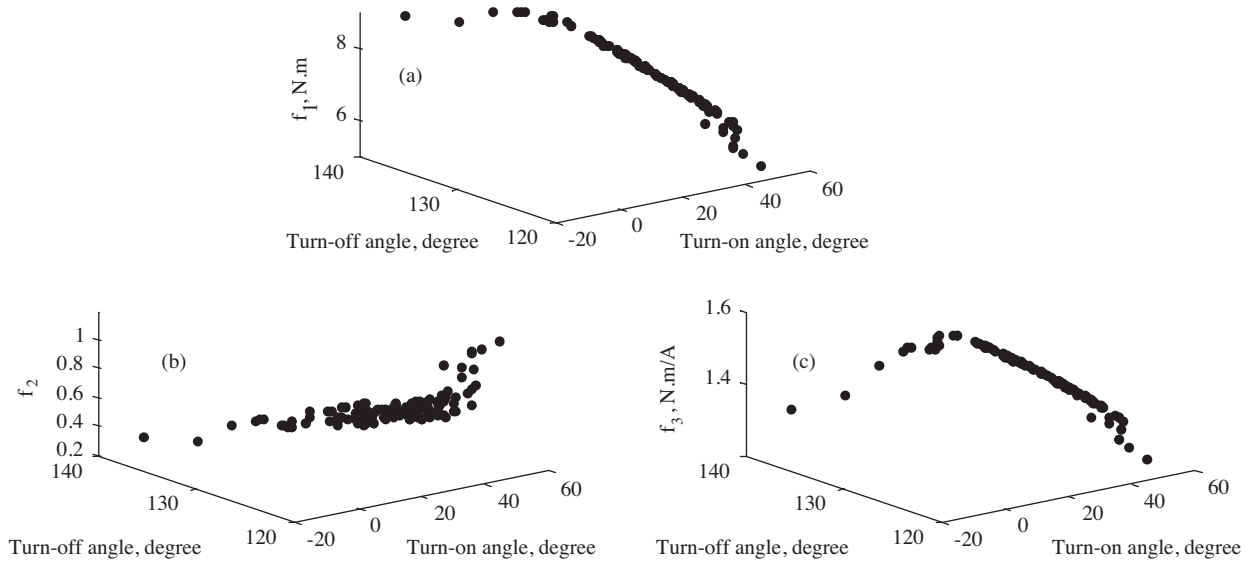

Figure 13. Values of decision variables θ_{on} and θ_{off}: a) versus objective function f_1, b) versus objective function f_2, and c) versus objective function f_3.

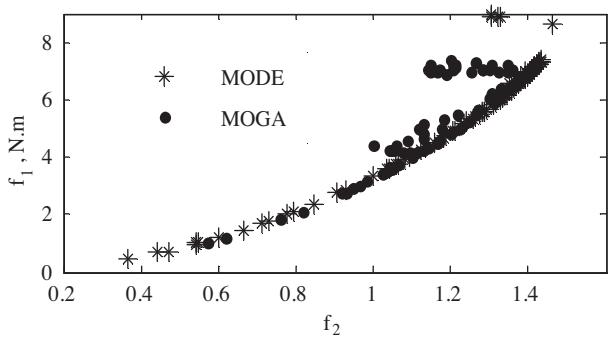

Figure 14. The performance of the MODE algorithm compared with the MOGA.

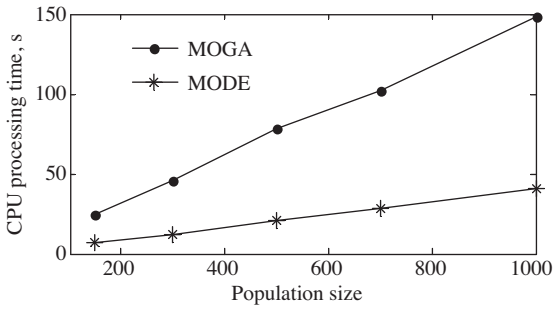

Figure 15. Processing time comparison between the MODE and MOGA algorithms.

4. Conclusions

The MODE algorithm was applied successfully to the multiobjective performance optimization of SRM drives. The optimum firing angles, turn-on and turn-off, achieving the maximum average torque with a low torque ripple and the maximum average torque per RMS current, were conducted on a 4-phase 4 kW motor drive and various results were demonstrated. The investigation on the motoring operation of the SRM drive has shown that the turn-on and turn-off angles have considerable effects on the criteria and that the turn-on and turn-off angles can be optimized to obtain the maximum average torque, maximum average torque per RMS current, and minimum torque ripple factor. This paper confirms the potential of the MODE to solve complex problems like the multiobjective optimization of SRM drives. Finally, it is suggested that the developed MODE algorithm can be used as an efficient alternative technique to solve multiobjective optimization engineering problems.

Nomenclature

V	Phase voltage
R	Phase winding resistance
i	Phase current
φ	Flux linkage
$\frac{d\varphi}{dt}$	Rate of flux linkage
W'	Coenergy
θ	Rotor angular position
T_e	Instantaneous developed total torque
T_{avg}	Average torque
τ	Time period
$\varphi(0)$	Flux linkage at time t = 0
P_{cu}	Copper loss
I_{rms}	RMS current
K_T	Torque ripple factor
$T_{e\max}$	Maximum value of instantaneous torque
$T_{e\min}$	Minimum value of instantaneous torque
TP	Average torque per RMS current
$\theta_{on}^{opt}, \theta_{off}^{opt}$	Optimal control parameters
$\theta_{on}, \theta_{off}$	Turn-on and turn-off angles
ω	Rotor speed
I_{ref}	Current reference
ω_b	Base rotor speed
P_r	Rated power
SRM_mc	SRM measured characteristics
D	Number of dimensions
NP	Population size
CR	Crossover constant
F	Scaling factor
G	Generation counter
NG	Maximum generation

References

[1] Z.Y. Zhen, W.M. Terry, C.B. Juan, "An investigation of multiphase excitation modes of a 10/8 switched reluctance motor with short flux path to maximize its average torque", Proceedings of the 9th IEEE International Symposium on Industrial Electronics, Vol. 2, pp. 390–395, 2000.

[2] A.D. Cheok, Y. Fukuda, "A new torque and flux control method for switched reluctance motor drives", IEEE Transactions on Power Electronics, Vol. 17, pp. 617–626, 2002.

[3] C. Changhwan, K. Seungho, K. Yongdae, P. Kyihwan, "A new torque control method of a switched reluctance motor using a torque-sharing function", IEEE Transactions on Magnetics, Vol. 38, pp. 3288–3290, 2002.

[4] J. Reinert, R. Inderka, M. Menne, R.W. De Doncker, "Optimizing performance in switched reluctance drives", IEEE Transactions on Industrial Application and Magnetics, Vol. 6, pp. 63–70, 2000.

[5] W. Shun-Chung, L. Wen-Han, "Turn-on angle searching strategy for optimized efficiency drive of switched reluctance motors", Proceedings of the 30th Annual Conference of the IEEE Industrial Electronics Society, Vol. 2, pp. 1873–1878, 2004.

[6] O. Seok-Gyu, A. Jin-Woo, L. Young-Jin, L. Man-Hyung, "Study on optimal driving condition of SRM using GA-neural network", Proceedings of the 10th IEEE International Symposium on Industrial Electronics 2001, Vol. 2, pp. 1382–1386, 2001.

[7] R.T. Naayagi, V. Kamaraj, "Minimization of torque ripple in switched reluctance machine for direct drive applications", Proceedings of International Conference on Emerging Technologies, pp. 388–392, 2005.

[8] N. Bhiwapurkar, N. Mohan, "Torque ripple optimization in switched reluctance motor using two-phase model and optimization search technique", Proceedings of the International Symposium on Power Electronics, Electrical Drives Automation and Motion, pp. 340–345, 2006.

[9] K.I. Hwu, C.M. Liaw, "Intelligent tuning of commutation for maximum torque capability of a switched reluctance motor", IEEE Transactions on Energy Conversion, Vol. 18, pp. 113–120, 2003.

[10] P.L. Chapman, S.D. Sudhoff, "Design and precise realization of optimized current waveforms for an 8/6 switched reluctance drive", IEEE Transactions on Power Electronics, Vol. 17, pp. 76–83, 2002.

[11] R. Gobbi, N.C. Sahoo, "Optimization techniques for a hysteresis current controller to minimize torque ripple in switched reluctance motors", IET Electric Power Applications, Vol. 3, pp. 453–460, 2009.

[12] J.M. Stephenson, A. Hughes, R. Mann, "Online torque ripple minimization in a switched reluctance motor over a wide speed range", IEE Proceeding of Electric Power Applications, Vol. 149, pp. 261–267, 2002.

[13] X.D. Xue, K.W.E. Cheng, J.K. Lin, Z. Zhang, K.F. Luk, N.C. Cheung, "Optimal control method of motoring operation for SRM drives in electric vehicles", IEEE Transactions on Vehicle Technology, Vol. 59, pp. 1191–1204, 2010.

[14] H. Yahia, M.F. Mimouni, R. Dhifaoui, "New control strategy of switched reluctance machine drives", International Review of Modelling and Simulation", Vol. 3, pp. 299–305, 2010.

[15] F. D'hulster, K. Stockman, J. Desmet, R. Belmans, "Advanced nonlinear modeling techniques for switched reluctance machines", International Conference on Modeling, Simulation and Optimization, pp. 44–51, 2003.

[16] T.J.E. Miller, M. McGilp, "Nonlinear theory of the switched reluctance motor for rapid computer-aided design", IEE Proceedings B - Electric Power Applications, Vol. 137, pp. 337–347, 1990.

[17] K. Vijayakumar, R. Karthikeyan, S. Paramasivam, R. Arumugam, K.N. Srinivas, "Switched reluctance motor modeling, design, simulation, and analysis: a comprehensive review", IEEE Transactions on Magnetics, Vol. 44, pp. 4605–4617, 2008.

[18] H.F. John, L. Yun, P.C. Kjaer, J.J. Gribble, T.J.E. Miller, "Pareto-optimal firing angles for switched reluctance motor control", Proceedings of the 2nd IEE/IEEE International Conference on Genetic Algorithms in Engineering Systems: Innovations and Applications, Vol. 3, pp. 1–6, 1997.

[19] M. Martin, H. Aleš, "Optimization of switched reluctance motor control", Proceedings of the 10th Conference Student EEICT, Vol. 3, pp. 484–487, 2004.

[20] D.A. Torrey, J.H. Lang, "Optimal-efficiency excitation of variable-reluctance motor drives", IEE Proceedings B - Electric Power Applications, Vol. 138, pp. 1–14, 1991.

[21] M.O. Avoki, "A new technique for multidimensional performance optimization of switched reluctance motors for vehicle propulsion", IEEE Transactions on Industrial Applications, Vol. 39, pp. 387–392, 2003.

[22] J.X. Xu, S.K. Panda, Q. Zheng, "Multiobjective optimization of current waveforms for switched reluctance motors by genetic algorithm", Proceedings of the World Congress on Computational Intelligence, Vol. 2, pp. 1860–1865, 2002.

[23] X.D. Xue, K.W.E. Cheng, T.W. Ng, N.C. Cheung, "Multi-objective optimisation design of in-wheel switched reluctance motors in electric vehicles", IEEE Transactions on Industrial Electronics, Vol. 57, pp. 2980–2987, 2010.

[24] F. Xue, A.C. Sanderson, R.J. Graves, "Pareto-based multi-objective differential evolution", Proceedings of the Congress on Evolutionary Computation, Vol. 2, pp. 862–869, 2003.

[25] B.V. Babu, P.G. Chakole, J.H.S. Mubeen, "Multiobjective differential evolution (MODE) for optimization of adiabatic styrene reactor", Journal of Chemical Engineering Science, Vol. 60, pp. 4822–4837, 2005.

[26] E.M. Montes, M.R. Sierra, C.A. Coello, "Multi-objective optimization differential evolution: a survey of the state of the art", Advances in Differential Evolution Studies in Computational Intelligence, Vol. 3, pp. 540–567, 2008.

[27] J.A. Adeyemo, F.A.O. Otieno, "Multi-objective differential evolution algorithm for solving engineering problems", Journal of Applied Sciences, Vol. 9, pp. 3652–3661, 2009.

[28] D.G. Regulwar, S.A. Choudhari, P.A. Raj, "Differential evolution algorithm with application to optimal operation of multipurpose reservoir", Journal of Water Resource and Protection, Vol. 2, pp. 560–568, 2010.

[29] L.V. Santana-Quintero, C.A. Coello, "An algorithm based on differential evolution for multi-objective problems", International Journal of Computational Intelligence Research, Vol. 1, pp. 151–169, 2005.

[30] M.J. Reddy, D.N. Kumar, "Multiobjective differential evolution with application to reservoir system optimization", Journal of Computing in Civil Engineering, Vol. 1, pp. 136–146, 2007.

[31] R. Storn, K.V. Price, "Differential evolution - a simple and efficient heuristic for global optimization over continuous spaces", Journal of Global Optimization, Vol. 11, pp. 341–359, 1997.

[32] B.V. Babu, J.H.S. Mubeen, P.G. Chakole, "Multi-objective optimization using differential evolution", Journal of Information Technology, Vol. 2, pp. 4–12, 2005.

[33] H. Yahia, N. Liouane, R. Dhifaoui, "Weighted differential evolution based PWM optimization for single phase voltage source inverter", International Review of Electrical Engineering, Vol. 9, pp. 125–130, 2010.

[34] K. Deb, "Multi-objective Optimization Using Evolutionary Algorithms", New York, Willey, 2001.

[35] K. Deb, S. Agrawal, A. Pratap, T. Meyarivan, "A fast elitist non-dominated sorting genetic algorithm for multi-objective optimization: NSGA-II", Proceedings of the 6th International Conference on Parallel Problem Solving from Nature, Vol. 3, pp. 849–858, 2000.

[36] H. Kung, F. Luccio, F. Preparata, "On finding the maxima of a set of vectors", Journal of the Association Computing Machinery, Vol. 22, pp. 469–476, 1975.

[37] K. Mishra, S. Harit, "A fast algorithm for finding the non dominated set in multi-objective optimization", International Journal of Computer Applications, Vol. 1, pp. 35–39, 2010.

[38] J. Du, Z. Cai, Y. Chen, "A sorting based algorithm for finding non-dominated set in multi-objective optimization", Proceedings of the 3rd International Conference on Natural Computation, Vol. 4, pp. 436–440, 2007.

[39] D. Swagatam, A. Ajith, K.C. Uday, K. Amit, "Differential evolution using a neighborhood-based mutation operator", IEEE Transactions on Evolutionary Computation, Vol. 1, pp. 526–553, 2009.